INTERNATIONAL JOURNAL OF CLIMATOLOGY
Int. J. Climatol. (2011)
Published online in Wiley Online Library
(wileyonlinelibrary.com) DOI: 10.1002/joc.3395

RMetS
Royal Meteorological Society

Estimation of trends in extreme melt-season duration at Svalbard

Nils Gunnar Kvamstø,[a]* Dag Johan Steinskog,[b] David B. Stephenson[c] and Dag Bjarne Tjøstheim[d]

[a] *Geophysical Institute, University of Bergen and, The Bjerknes Centre for Climate Research, Bergen Norway*
[b] *Nansen Environmental and Remote Sensing Centre and The Bjerknes Centre for Climate research, Bergen, Norway*
[c] *School of Engineering, Computing and Mathematics, University of Exeter, UK and Geophysical Institute, University of Bergen, Norway*
[d] *Institute of Mathematics, University of Bergen, Norway*

ABSTRACT: A time series of monthly mean surface temperatures taken at Svalbard airport, Spitzbergen, for the period 1912–2010 was examined for changes in melt-season length. The annual melt-season length was constructed from daily temperature estimates based on the monthly data using smoothing splines. We argue that the changes in annual melt-season length are linked to variability in regional sea surface temperatures, the mean Northern Hemisphere surface temperature and the North Atlantic Oscillation (NAO) index. A regression model for the melt-season length with these three parameters as predictors, explained about 40% of the observed variance. The annual mean melt season for the period from 1912 to 2010 was estimated to be 108 days, and the linear trend was 0.17 days/year. The risk of having positive extremes in the melt season increased with increasing Northern Hemisphere surface temperature and the regional sea surface temperatures. On the basis of our study of past observations, the 100-year return length of the melt season at Svalbard was predicted to change from the current 95% confidence interval of 131 (108, 138) days to 175 (109, 242) days with 1 °C warming of both regional sea surface temperature and the mean Northern Hemisphere surface temperature.

KEY WORDS melt season; length; trends; extremes; Arctic; Spitzbergen

Received 23 April 2010; Revised 9 September 2011; Accepted 9 October 2011

1. Introduction

The Arctic, defined as the region north of 60 °N, has undergone a warming trend in the past 100 years that is twice the global observed warming trend (ACIA, 2005; IPCC WG1 FAR, 2007). The annual mean temperature has risen 0.09 ± 0.03 °C per decade during the period between 1875 and 2000 (Polyakov *et al*., 2002). While the warming trend has been most pronounced in the winter and spring, all seasons have experienced an increase in temperature over the past several decades (ACIA, 2005). However, strong decadal variations are present (Polyakov *et al*., 2003). There are also spatial variations. Rigor *et al*. (2000) showed that during winter, in the period 1979–1997, there were a warming trend in the Eastern Arctic and a slight cooling trend in the Western Arctic. In spring, there is a relatively uniform warming trend in the Arctic, whereas in summer and autumn we find weaker and more scattered changes. An exception in the latter season is a warming trend in the Arctic Pacific. There are spatio-temporal changes in Arctic snow cover, but on average the spring snow cover melted 4–7 days earlier during the last two decades or so as compared to the two preceding decades (Foster *et al*., 2008).

Rather than assessing the risk of an extremely warm period in the Arctic based on the conventional analysis of monthly temperature records, the aim of this study is to take an alternative approach and investigate the behaviour of the melt-season length at an Arctic station from 1912 to 2010. Comisio (2003) showed that there was a positive trend in the Arctic melt season during the period 1981–2001. He also showed that there was a considerable spread between different Arctic regions, but all of them were positive. Internal climate variability in the Arctic operates on a wide range of time scales, and a long sampling time is required to obtain a signal-to-noise ratio with an acceptable level of certainty (Sorteberg and Kvamstø, 2006). Decadal variations are well within the internal variability regime and thus the representativeness of a 20-year period will be associated with a considerable level of uncertainty. With this background, we will examine variability and trends over a longer period. Owing to the sparseness of instrumental data in the Arctic, we will not examine geographical differences in this paper.

The physical implications of longer melt periods can be dramatic. In the marginal ice zone during the summer, the ice was assumed to have little or no snow cover. A

* Correspondence to: N. G. Kvamstø, Geophysical Institute, University of Bergen, Allegaten 70, N-5070 Bergen, Norway.
E-mail: Nils.Kvamsto@gfi.uib.no

typical value of the surface albedo under such circumstances is 30% (Hartmann, 1994 (p. 88)). The long-term (1984–2008) downward shortwave radiation at the surface for July (Hatzianastassiou *et al.*, 2005) shows a value of 200 Wm^{-2} in the area of interest for this research. In this case, the meltdown of a fully ice-covered surface implies an extra heat source of 40 Wm^{-2} into the ocean, assuming an open water albedo of 10%. The Arctic Ocean in the summer generally has a sea-ice fraction value of less than 1. Still, enhanced melting could cause a positive feedback contribution of approximately 20 Wm^{-2}. Such an increase in the heat source for the upper ocean can lead to a delayed occurrence of sea ice in the autumn and earlier melting during the spring. A substantial increase in the length of the melting period could thus trigger the ice albedo feedback, leading to a drastic reduction in the Arctic sea-ice extent and a regime shift in Arctic temperatures.

An increase in melt-season length has several important consequences, such as a reduction in the permafrost (ACIA, 2005; Hinzman *et al.*, 2005; IPCC WG2 FAR, 2007) and a lengthening of the growing season, resulting in changes in vegetation and ecology (Smith *et al.*, 2004; Loeng *et al.*, 2005). With these expected and ongoing changes (Serreze *et al.*, 2009), the whole appearance of the Arctic will be altered. Permafrost, for instance, is recognized as solid ground for construction, but warming will make construction and infrastructure more vulnerable (IPCC WG2, 2001; ACIA, 2005). Moreover, coastal erosion will be a growing problem as rising sea levels and reductions in sea ice allow higher storm surges to reach the shore. However, there might be consequences that could be beneficial to parts of the region as well. One of the positive impacts of early Arctic melt is the opening up of the Northern Sea Route, or the Northeast Passage, for ship transportation (Johannessen and Pettersson, 2008). It will also offer greater access to gas, oil, seabed mineral resources as well as the possibility of expanded commercial fishing. This has lead to increased human activity and interest in the area and there is a growing awareness of the strategic importance and nature of this unique region. This background furnishes ample motivation for the study of changes in the melt-season length.

The aim of this study is to develop and test a robust methodology for investigating trends and variations in melt-season length. Extreme value theory models are used to estimate the risk of an extremely long melt season, which are highly relevant to global warming impact in the Arctic. We focus here on large-scale physical parameters that can be well represented in global climate models (GCMs). Many regional- and fine-scale quantities might provide additional physically relevant information, but these are associated with a higher level of uncertainty in GCM simulations (Sorteberg *et al.*, 2005).

A brief summary of the paper is as follows. The physical mechanisms behind the variations in melt-season length are discussed in Section 2, while the data are presented in Section 3. The methodology behind the reconstruction of the melt season and temporal variation is described in Section 4. The modelling of mean melt-season length is given in Section 5, and a risk assessment is given in Section 6. Conclusions are presented in Section 7.

2. Physical processes

We used the atmospheric energy budget equation as a framework for discussing parameters that can represent the physical processes in our statistical models. Low-level energy variations are closely related to low-level temperature variations. In this work, we assumed that the temperature was well correlated with melt-season length (this is discussed further in Section 4). The local energy budget equation of an atmospheric column of unit horizontal area can be written as

$$\frac{\partial A_E}{\partial t} = -\nabla \cdot F_{AE} + R_A + LP + SH \qquad (1)$$

Where A_E is the atmospheric energy in the column, R_A is the net radiative heating of the atmospheric column, LP is the heating of the atmospheric column by latent heat release during precipitation, SH is the sensible heat transfer from the surface to the atmosphere and $(-\nabla \cdot F_{AE})$ is the horizontal divergence of energy in the column by the atmospheric circulation. From the definition of A_E it follows that

$$\frac{\partial A_E}{\partial t} = \frac{\partial}{\partial t}\left[\frac{1}{g}\int_0^{p_s}(c_pT + \Phi + Lq + k)dp\right] \qquad (2)$$

where p is pressure, p_s is surface pressure, c_p is the specific heat of dry air at constant pressure (1005.7 $\mathrm{J\ K}^{-1}\ \mathrm{kg}^{-1}$), T is temperature, k is kinetic energy, L is latent heat of evaporation ($2.501{\cdot}106\ \mathrm{J\ kg}^{-1}$), q is specific humidity, g is the gravitational acceleration (9.81 ms^{-2}) and Φ is the geopotential. The sum of the first two terms in the parentheses of Equation (2) is called the dry static energy, while the sum of the first three terms is called the moist static energy.

The long-term average of the storage term in the Arctic region is small ($\sim$25 Wm^{-2}) but positive in the summer season (Serreze *et al.*, 2007). The interannual and decadal variability of the storage term is nearly an order of magnitude smaller than the seasonal variation. A more detailed analysis of the Arctic energy budget is available in Serreze *et al.* (2007).

The poleward heat transport tends to be dominated by the synoptic part of the flow but still has significant contributions from the mean meridional circulation and the quasi-stationary eddies (Hartmann, 1994 (Ch.6)). On the basis of wintertime data, Seierstad *et al.* (2007) have shown that there is a substantial degree of correlation between synoptic storminess and large-scale flow indices. To our knowledge, very few studies have explored summertime synoptic activity, except for Mesquita (2006) and Serreze *et al.* (2000). Mesquita (2006) has shown

that there is some indication that teleconnection indices based on NCEP data (Wallace and Gutzler, 1981; Barnston and Livezey, 1987) are linked to summer storminess in the North Atlantic and Nordic Seas. In our statistical model (Sections 5 and 6), we thus let large-scale circulation indices represent the effect of atmospheric transport or advection.

Low frequent changes in the wind pattern may also drastically affect the sea-ice conditions and, in turn, the low-level temperatures (through *SH* and *LP*) (Smedsrud *et al*., 2008). Belchansky *et al*. (2004) have shown that the winter Arctic Oscillation (AO) index is correlated with sea-ice extent in the following summer. After a high-index AO winter (January–March), they found that the spring melt tended to be earlier and the autumn freezing tended to be later, leading to a longer melt season. The connection was strongest for the Siberian Arctic region and was caused by cyclonic activity and associated ice drift anomalies during a high phase of the AO index. The winter AO index, or a similar leading mode, can therefore also be a candidate for a sea-ice proxy and thus represents the effect of *SH* and *LP* in our framework.

Francis and Hunter (2007) showed that regional sea surface temperatures (SST) can explain up to 20% (depending on accumulation time) of the variance in winter sea-ice extent in the Barents Sea. This is close to Svalbard and strongly suggests regional SSTs to be a potentially important factor and proxy for surface fluxes. In their study of the impact of atmospheric variables on Arctic summer sea-ice extent, Francis and Hunter (2006) also found low-level winds to be an explanatory factor. They pointed out that the AO index could account for the low-level wind effect. This strengthens the candidateship for the AO- or NAO-index to represent the effect of the atmospheric flow variations.

In simple radiation balance models, R_A can be directly linked to the global mean temperature (i.e. Ramanathan *et al*., 1989). When allowing a time-dependent radiative forcing in such models, it is readily shown that the temperature response can be linearly related to the forcing (i.e. Hartmann, 1994; Schwartz, 2007). The global mean temperature could thus represent the bulk thermodynamic changes due to long-term variations and changes in the radiative forcing. Alexeev *et al*. (2005) have shown that Arctic amplification is inherently linked to mean global forcing. On the basis of this, we assumed that global or hemispheric mean temperature changes can represent the effect of radiative forcing (R_A) on the local temperature conditions.

3. Data

In this paper, the homogenized time series of monthly mean observed surface temperature for the period from 1912 to 2010 at Svalbard airport, Spitzbergen, were used (Nordli and Kohler, 2004; Nordli, 2010). Svalbard airport is located in the Arctic, according to all possible definitions given in the ACIA (2005). This time series is a composite of several adjusted shorter series of measurements at a few nearby sites. All the shorter time series have been adjusted (Nordli and Kohler, 2004; Nordli, 2010) so that they are valid for the current Svalbard airport weather station (78°150′N, 15°280′E, 28 m a.s.l.), which was established in 1975 (location indicated in Figure 1). This location is several kilometres away from Longyearbyen, where most of the infrastructural development has taken place during the last decades. Only a few modest changes in surface properties have taken place near the station. The minor actions taken to keep the homogeneity of the time series are described in Nordli (2010). The daily time series from 1975 to 2006 is also available and was used for validation purposes; however, daily data are not available for the period prior to 1975.

The homogenized Svalbard airport series is one of only a few long-term (>65 yr) and continuous instrumental temperature series from the high Arctic (Przybylak, 2003). The border of the Arctic ice sheet is the region where the projected largest changes in melt season are expected based on the IPCC WG1 FAR (2007). Svalbard

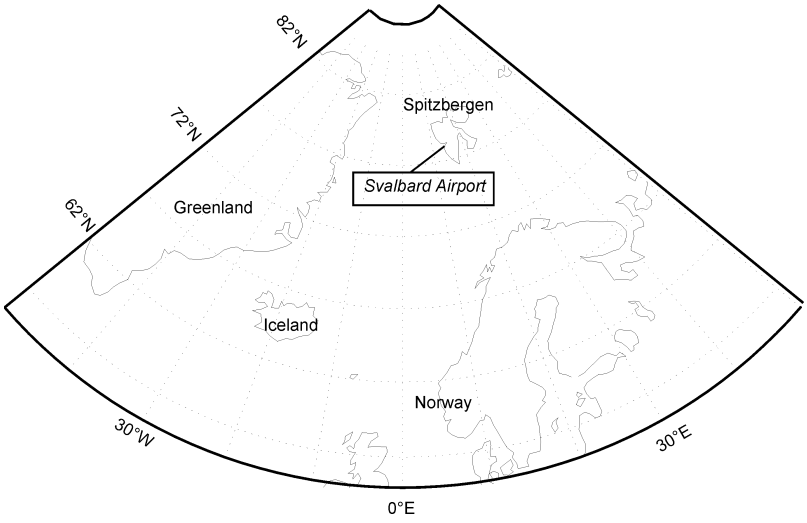

Figure 1. Geographic map of the Atlantic Arctic sector showing the location of Svalbard airport.

airport is in Spitsbergen, which is located close to the sea-ice border and should thus be a representative location that was utilized to investigate the trends in the melt-season length.

The Northern Hemispheric mean monthly 2-m air temperature anomalies (from the 1961–1990 mean) HadCRUT3v were also used and can be downloaded from the website http://www.cru.uea.ac.uk/cru/data/temperature/ (Jones *et al*., 1999). This dataset is one of many available global hemispheric temperature datasets, the properties of which do not differ greatly (IPCC WG1 FAR, 2007). Monthly mean SST anomalies averaged over the region 0°–30 °E and 66°–74 °N were provided from the HadISST1 dataset (Rayner *et al*., 2003).

We let large-scale atmospheric indices represent the effect of the atmospheric circulation. Two sets of indices that cover the full period of our temperature record were investigated. One was provided by Casty *et al*. (2007). We explored the first three principal components of combined monthly geopotential height, including: 500 hPa, surface temperature and precipitation fields. The principal components were based on reconstructed gridded monthly data taken since 1766 for all seasons in Europe (30°–80 °N, 50 °W–40 °E). For more details, see Casty *et al*. (2007). The subsequent analysis showed that only one of the three principal components was relevant in our case, namely the NAO-like second principal component.

We obtained similar results with a more standard NAO index introduced by Li and Wang (2003) based on standardized difference in zonal mean pressure between 65 °N and 35 °N in the North Atlantic sector. Index data downloaded from http://www.lasg.ac.cn/staff/ljp/data-NAM-SAM-NAO/NAO.htm (Li and Wang, 2003), show that this index is a more optimal representation of the spatial temporal variability associated with the NAO concerning explained fraction of variance, correlation strength and area size of correlation patterns. The last issue is of particular concern in this case as Spitzbergen is on the margin of the correlation patterns of some of the point-based indices. The area of the chosen index is large and covers well the region of interest here. In the following, we only show results obtained with this index. More detailsare given in (Li and Wang, 2003).

4. Reconstruction of melt-season time series and temperature variations

Here, we define the length of the melt season, τ, as the accumulated number of days when the daily surface temperature $T > 0$ °C and add the constraint that T must be greater than 0 °C for four days or more in a row to contribute to τ. To obtain daily values of surface temperature based on monthly time series (to estimate τ), smoothing splines were introduced (de Boor, 1978). Other methods are available (Epstein, 1991), but the smoothing spline is preferred because the harmonic fit suggested by Epstein (1991) involves the estimation of 12 parameters, while only 1 is required for smoothing splines. One way to estimate the smoothing parameter is to use degrees of freedom, a_{df} (Green and Silverman, 1993). The results of the smoothing spline method adapted for monthly values were compared with daily observations for 2006, as shown in Figure 2. The daily observations were expectedly noisier than the reconstructed daily values. The smoothing parameter $a_{df} = 15$ was estimated by minimising the difference between the observed and reconstructed τ for the Svalbard airport between 1976 and 2006. It should also be mentioned that the best fit between these estimates was obtained with the additional constraint that $T > 0$ °C in four days or more in a row to contribute to τ.

The reconstructed and observed annual τ at Svalbard airport is shown in Figure 3(a) for the full period. The

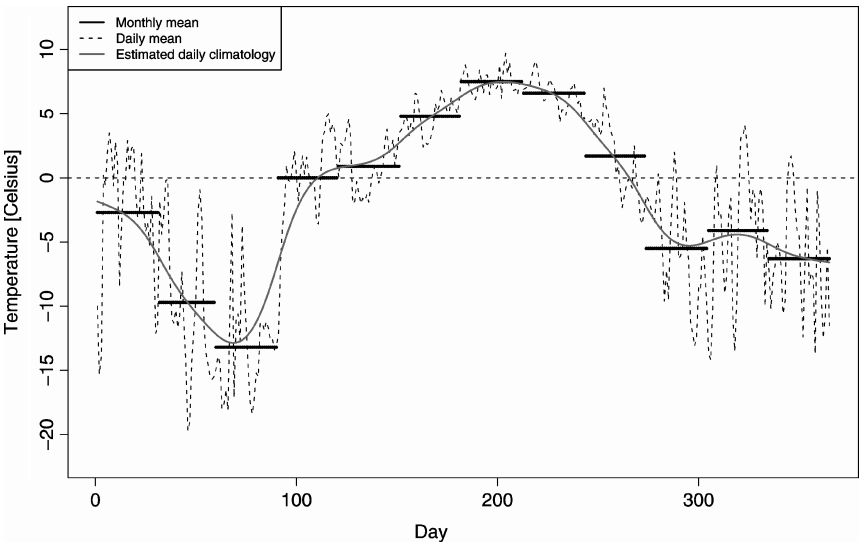

Figure 2. Dashed line: Observed daily evolution of temperature at Svalbard Lufthavn in 2006. Solid grey line: Estimated daily values for the same period, with the application of smoothing splines (see text). Black solid line segments: Observationally based monthly mean temperature for 2006.

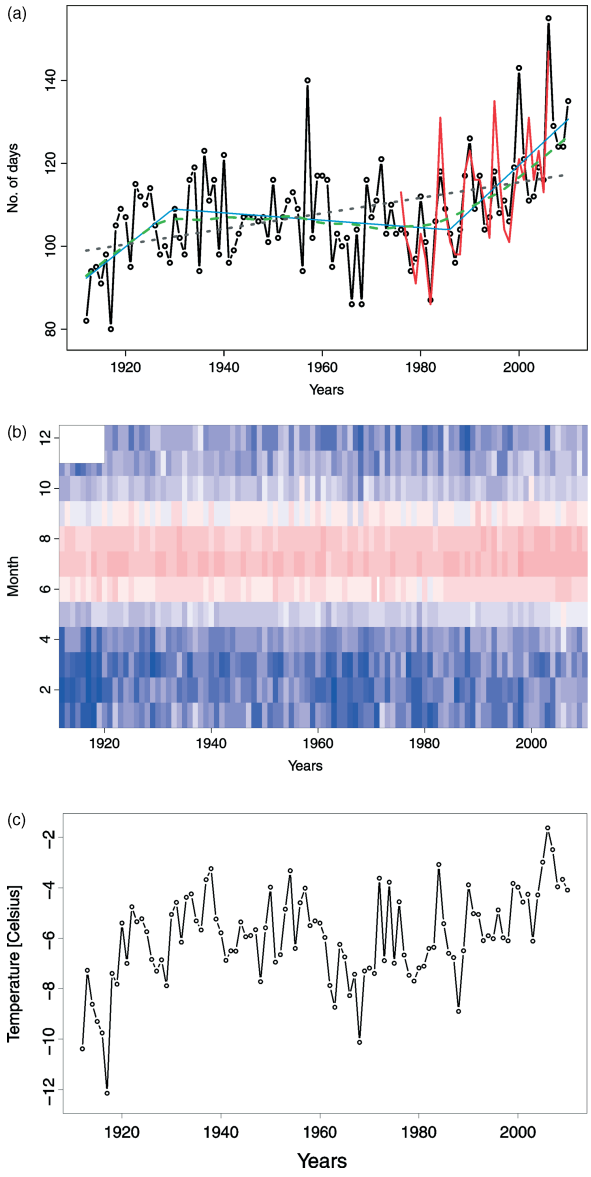

Figure 3. (a) Black solid line: Time series of the melt-season length, τ, estimated from monthly temperature records at Svalbard Airport, Spitzbergen. Red solid line: Observed τ using daily data from Svalbard Airport for the period 1976–2006. Blue solid line: Segmented regression. Green dashed line: Nonlinear trend with Lowess. Grey dashed line: Linear trend. (b) Monthly temperature variations at Svalbard airport. (c) The time series of annual mean temperature at Svalbard airport.

mean melt-season duration for the period from 1912 to 2010 was estimated to be 108 days, and the linear trend was 0.17 ± 0.04 days/year. The estimated trends in this section are given with a 95% confidence interval. These results are in accordance with Rigor *et al.* (2000), who reported that the marginal ice zone has around 100 days of melt-season duration. This result is also in agreement with findings in Markus *et al.* (2009) and Kaufman *et al.* (2009). The estimated trend was quite similar to the change in growth season over the same period (IPCC WG1 FAR, 2007), which was between 1 and 3 days per decade depending on the location in the Arctic. However, there was a large decadal variation. A fitted segmented linear regression (Muggeo, 2003) gives a growing trend in τ for the period 1912–1929 (0.95 ± 0.46 days/year), a decreasing trend for the period 1930–1985 (-0.09 ± 0.08 days/year) and a new increasing trend for the period 1986–2010 (1.11 ± 0.28 days/year). Note that the breaking points were determined by the segmentation algorithm. There was good agreement between the segmented linear trend and the nonlinear lowess (Cleveland, 1979, 1981) (Figure 3(a)). A paired two-sample t-test with a removed linear trend over the period 1976–2006 indicates that there was not a significant difference between the observed and reconstructed τ. For the period from 1976 to 2006, the development of the estimated annual τ adequately resembled the observations, with a few exceptions (Figure 3(a)). Figure 3(b) shows the seasonal temperature cycle at Svalbard airport for each year in the record. It is evident that the melting intervals occurred more frequently in the fall towards the end of the record.

The assumption that the processes governing the mean local atmospheric energy budget (and temperature) can also be tied to the melt-season length rests upon the existence of a close link between annual/seasonal temperature and annual/seasonal melt-season length. As τ was constructed from temperatures at the warmest part of the year, it is not obvious that it is directly related to the mean temperature over that period. There is, for example, a possibility that the melt season is short with a higher than normal mean temperature. This implies that the cold part of the period would be anomalously warm, but not higher than 0 °C. The link between melt-season length and temperature is briefly examined in the following section.

The annual mean temperature $\overline{T_S}$ in the period from 1912 to 2010 was −6.0 °C. A segmented regression analysis (Muggeo, 2003) showed a significant trend of $0.22^{\circ} \pm 0.11$ °C/year for the period 1912–1931, -0.04 ± 0.03 °C/year in the period 1932–1978, and 0.12 ± 0.05 °C/year for the period 1979–2010. There are many similarities between these data and the time evolution of τ (Figure 3(a) and (c)). The breaking points occurred roughly at the same time, and the empirical correlation was computed to be 0.734. Przybylak (2003 (p. 63–81)) has shown that the Arctic winter temperature has a higher variability than the summer temperature over a wide range of scales. This is presumably due to more vigorous atmospheric dynamics during winter and the damping effect of the energy-consuming melt process in summer. This strongly suggests that the winter period should be omitted when exploring the behaviour of the melting period length and processes explaining its variability.

Thus, the temperature for the warm season (AMJJAS) was extracted together with the respective estimated melt-season length, τ^s. The difference between τ and τ^s is that τ was based on annual observations, while τ^s was based on data from the warm season only. It was found that the empirical correlation between the mean summer temperature $\overline{T_S^s}$ and τ^s was 0.800. To illustrate the connection between temperatures and melt-season

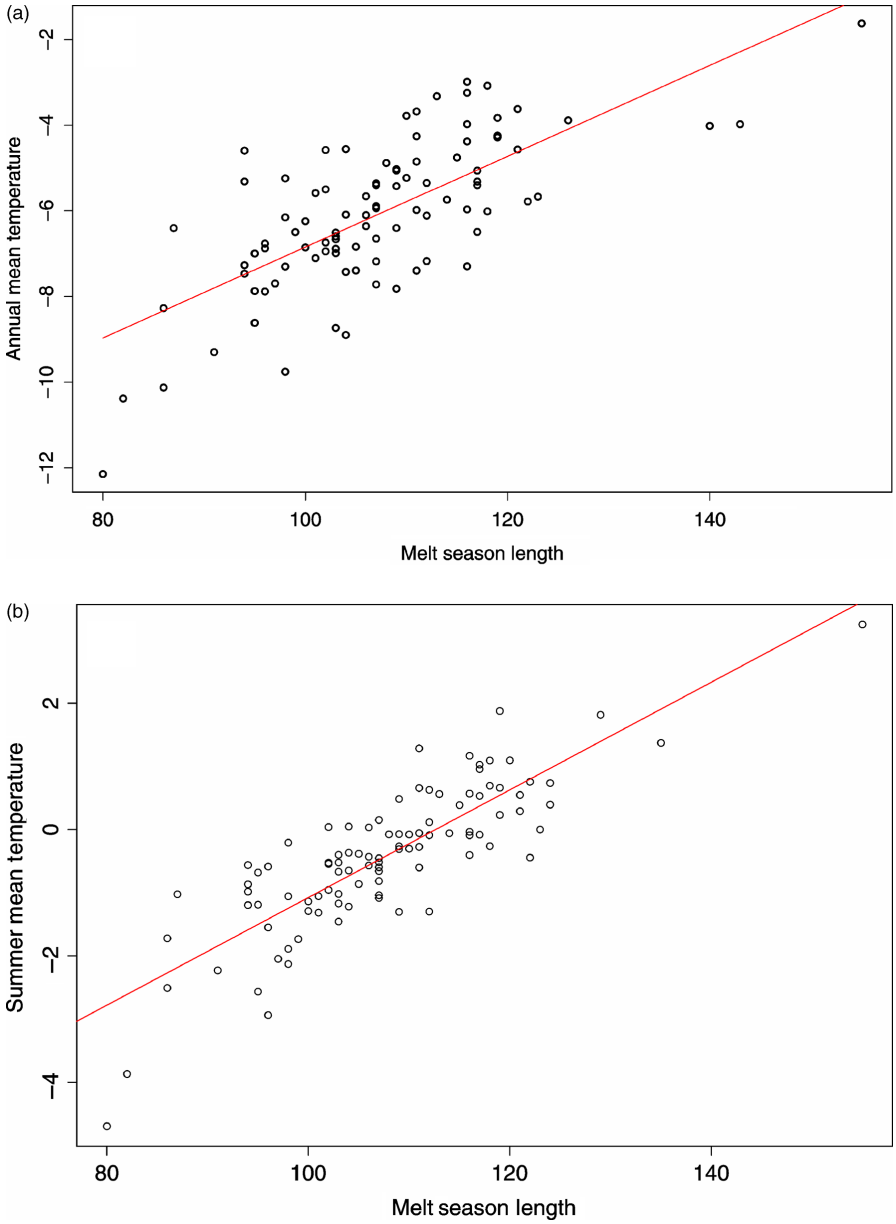

Figure 4. Scatterplot (a) between annual surface temperatures at Svalbard airport and melt-season length τ. The straight line is the linear regression line. (b) Same as in (a), but between the mean surface temperature and melt-season length τ^s in the warm season (AMJJAS). This figure is available in colour online at wileyonlinelibrary.com/journal/joc

length for the whole year and warm season, two scatter plots of the two variables are included in Figure 4(a) and (b). As indicated by the empirical correlation above, we found a close correspondence between the melt season and temperature, particularly for the summer.

The melt-season lengths τ and τ^s were not significantly different. When examining the date of the first and last annual event with $T_{4,daily} > 0\,^{\circ}\mathrm{C}$, we found that the longest melt seasons mostly had contributions from warm days that occurred later than normal in the year. The only exception was the melt-season peak in 2006, which was caused by an early spring heat spell. Thus, we conclude that the positive trend in melt-season length τ is mainly caused by an increased frequency of warm periods in the fall (September and October). Therefore, the melt season τ was used in the rest of the study to avoid missing any warm periods that might have occurred outside of the summer months.

5. Mean melt-season variability

To obtain indications of which processes affect the melt-season change at Svalbard, we employed a linear regression model where τ was linearly related to the set of predictors that were discussed in Section 2. In Section 2, a discussion of the local energy balance provided variables that may have had an impact on the temperature and therefore also on τ.

On the basis of the discussion in Section 2, we represented the impact of the large-scale flow variations using the NAO index from Li and Wang (2003). The radiative

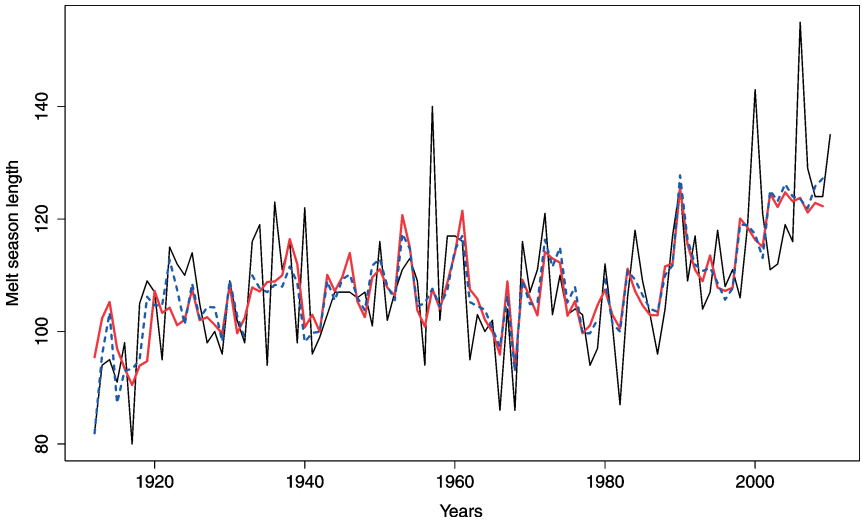

Figure 5. The time series of τ. Black solid line: Observationally based. Red solid line: Modelled τ (Equation (2)). Blue: Modelled τ in 3 sub-periods separately. Blue dashed line (1912–1929), blue dotted line (1930–1985), and blue dash-dotted line (1986–2010).

forcing R_a was represented by the Northern Hemisphere temperature anomaly, and as a third predictor, we used the annual regional SST anomaly in the Norwegian Sea to represent the effect of surface properties. The relevant regression model then becomes

$$\tau = \alpha + \beta_1 T_{gnh} + \beta_2 NAO^s + \beta_3 NAO^w + \beta_4 SST + \varepsilon$$
$$\varepsilon \sim N(0, \sigma_\varepsilon) \quad (3)$$

Where τ is the length of the melt period, T_{gnh} is the annual Northern Hemispheric temperature anomaly, NAO^s and NAO^w are the mean summer (JJA) and preceeding winter (DJFM) NAO indices, respectively. *SST* is the annual SST anomaly in the Norwegian Sea. The parameters were estimated to be (with a 95% confidence interval): $\alpha = 105.4 \pm 2.7$, $\beta_1 = 14.2 \pm 8.4$, $\beta_2 = 3.7 \pm 3.6$, $\beta_3 = 0.0 \pm 1.1$, $\beta_4 = 16.0 \pm 6.3$, and $\sigma_\varepsilon = 9.3$. The proportion of the total variance of τ, as explained by a linear relationship, was estimated to be $R^2 = 0.401$.

Dominance analysis (Budescu, 1993; Azen and Budescu, 2006) showed that the order of dominance (ranging from most important to least important) is *SST*, T_{gnh}, NAO^s and NAO^w. We interpret the impact of SST here to be connected with the negative correlation between sea-ice extent anomalies and SST anomalies found in this region (Bengtsson *et al*., 2004; Sorteberg and Kvingedal, 2006; Francis and Hunter, 2007). A rise in regional SST has a direct effect on surface air temperature and τ, but the indirect effect by exposing Arctic air-masses to larger areas of open waters will contribute significantly as well. As NAO can be seen as the Atlantic manifestation of the hemispheric AO, this finding is supported in Belchansky *et al*. (2004) as they reported a link between strong wintertime AO and longer melt seasons the following summer. The τ-values predicted by Equation (3) are shown in Figure 5(a). The low-frequent variability in τ was nicely explained by the model. When τ was smoothed by the lowess method (Cleveland, 1981, 1979), the proportion of the total variance of τ explained by a linear relationship increases, confirming that the model agreeably explains the low-frequency changes in τ. However, extreme events, and to some degree interannual high-frequency variability, were not well explained. A closer inspection of the parameter distribution in some of the extreme years shows in general that extremely high/low τ values are not caused by extreme values in one of the parameters, but is rather a result of a combination of more moderate parameter values. This illustrates that the melt-season length is a quantity that integrates many processes. Atmospheric thermal effects throughout the year, the preceding winter circulation, its mechanical forcing of the sea ice, surface fluxes and short-term cloud-radiative effects are processes at play. Thus, a far more complex model with detailed model input is required to simulate the short-term fluctuations.

6. Risk of extremely long melt seasons

As stated in the introduction, it is of vital importance to evaluate the risk of extremely long melt seasons. The average melt season at Svalbard was 108 days over the 1912–2010 period. The highest value observed was 155 days (in 2006). Since the model presented in Equation (2) explained the gross development of τ over the record, we tested the predictors as covariates in an extreme value model. The covariates in the model, which added significant contribution, were *SST* and T_{gnh}. A likelihood ratio test (Coles, 2001; Coelho *et al*., 2008) was used in the testing.

Extreme events were defined as excesses above a high given threshold. The excesses can be modelled using the generalized Pareto distribution (GPD) (Coles, 2001). The threshold approach has been previously applied to tropical and extratropical climate data (Naveau *et al*., 2005; Nogaj *et al*., 2006; Coelho *et al*., 2008).

In the asymptotic limit for sufficiently large thresholds u, the distribution of excesses $z = \tau - u$ conditional on

$\tau > u$ can be shown to approximate the GPD function

$$\Pr(Z \leq z | Z > 0) = H(z) = 1 - (1 + \frac{\xi z}{\sigma})^{-\frac{1}{\xi}} \qquad (4)$$

which is defined for $z > 0$ for $\xi > 0$ and $0 \leq z \leq -\frac{\sigma}{\xi}$ for $\xi < 0$, where $\sigma > 0$ is the scale parameter and ξ is the shape parameter of the distribution. The scale parameter σ provides an estimate of the variability of the excesses. High values of σ have a higher variability of extremes. The shape parameter ξ provides information about the tail shape of the distribution of excesses. With covariates it is possible to identify factors that have an influence on the shape and scale parameters (Coles, 2001; Coelho *et al*., 2008). For a broader introduction to extreme value theory (EVT), refer Coles (2001).

An exponential link function was used to ensure that positive values of the scale parameter were obtained. The shape and scale parameters were estimated using maximum likelihood. The exponential link model is defined as

$$\log\ \sigma = \sigma_0 + \sigma_1 T_{gnh} + \sigma_2 SST \qquad (5)$$

$$\xi = \xi_0 \qquad (6)$$

Where ξ and σ are the shape and scale parameters in Equation (4). Because the data were not stationary, a time-varying threshold was applied. A smoothed non-parametric quantile regression (Koenker, 2005) with *SST* and T_{gnh} as covariates was used to estimate the threshold. Following Coles (2001 (p. 83–90)) for the choice in threshold where the asymptotic assumption of the Pareto distribution is valid, the ξ parameter should in theory be constant, while the σ parameter changes according to the formula

$$\sigma_u = \sigma_{u0} + \xi(u - u_0) \qquad (7)$$

where u and u_0 are two different thresholds with $u > u_0$ (Coles, 2001 (p. 83)). In Figure 6(a) and (b), the variability in ξ and σ are given as a function of the quantile threshold. The ξ parameter was fairly stable up to the 0.70 quantile, and the σ parameter decreased as expected because $\xi < 0$.

Generally, a threshold that is too low will violate the asymptotic assumptions of the GPD leading to a bias. On the other hand, a threshold that is too high will generate few excesses, leading to high variance. For the Svalbard airport time series, the threshold was set to be the 0.70 quantile as a compromise between bias and few excesses. This also seems reasonable in view of Figure 6.

The parameters in Equations (5) and (6) were estimated to be $e^{\sigma_0} = 7.51$ (4.97, 11.33), $e^{\sigma_1} = 1.90$ (0.63, 5.68), $e^{\sigma_2} = 1.51$ (0.69, 3.29) and $\xi_0 = -0.12$ (-0.36, 0.13) by the maximum likelihood method. The 95% confidence interval of ξ_0 shows that the excesses can have an unbounded distribution (cf. the domain of definition for Equation (4)). However, the evidence for ξ_0 being negative is reasonably strong because most of the domain of ξ_0 is negative. The probability and quantile plot were constructed as diagnostic model checks (Figure 7(b) and (c)) (cf. Coles, 2001 (p. 37)). These figures show few departures from the diagonal, thus lending support to the fitted model.

The excesses are shown in Figure 7(a). The excesses were approximately uniformly distributed in time. Exceptions included the melt seasons in 2006, 2000, and 1957, which stood out as extremely high excesses. The event in 1957 shows that there is a chance of having an extreme long melt season, despite lower values of T_{gnh} and a moderately positive *SST* (0.3 °C).

As shown in Sorteberg and Kvamstø (2006), there is a far larger spread in projected Arctic warming than projected global (or hemispheric) warming. We therefore concentrate here on the excesses' dependency on T_{gnh}. Figure 8(a) shows a scatter plot of the excesses and the T_{gnh} together with the median (solid line) and the upper/lower quartiles (dashed lines) of the GPD with the estimated shape and scale parameters. The increased variability in excesses can be noted for larger T_{gnh}. The T_{gnh} values utilized were deviations from the 1961–1990 mean. The mean threshold u for this period was estimated to be 111.2 days. The highest value of the threshold was 121.6 days for 2006. As noted in the formulation of Equation (4), the maximum upper bound of an excess was given as $z = \eta = -\frac{\sigma}{\xi}$ if $\xi < 0$. Assuming the estimated values of σ and ξ given above, the theoretical maximum upper bound of the excesses was estimated to be $\eta = 64.5$, resulting in an upper limit of $\tau_{max} = 175.7$. This was obtained by summation of the maximum upper limit of the excess and the mean of the 1961–1990 time varying threshold. The 95% confidence interval for ξ indicates that there is a chance that $\xi > 0$, in which case η may be exceeded. Therefore, the 100-year return level was investigated to check the risk of a long melt season with higher T_{gnh} (Figure 8(b)) and regional *SST*. A return level is a certain level of τ that is expected to be exceeded once in a given period. The 95% confidence interval of the return level was calculated based on the delta method (Coles, 2001 (p. 33)). Keeping SST constant to 0 °C, the confidence interval increased with T_{gnh} due to the relatively high value of σ_1 in the exponential link model (Equation (5)). We found that the 100-year return level increased with higher values of annual T_{gnh}, making the risk of large τ higher from 131 (108, 138) days when $T_{gnh} = 0$ °C to 140 (122, 158) days when $T_{gnh} = 0.5$ °C. The plot was extended up to $T_{gnh} = 1.0$ °C, which is a temperature increase that is expected to take place this century (IPCC WG1 FAR, 2007). The 100-year return level was 153 (98, 206) days for this case, an increase of 22 days from $T_{gnh} = 0$ °C. A similar increase was obtained by an additional warming of the regional *SST*. More specifically, for $T_{gnh} = SST = 1.0$ °C, the 100-year return level was 175 (109, 242) days. For $T_{gnh} = 1.0$ °C, $SST = 2.0$ °C, the 100-year return level raised to 210 (76, 343) days.

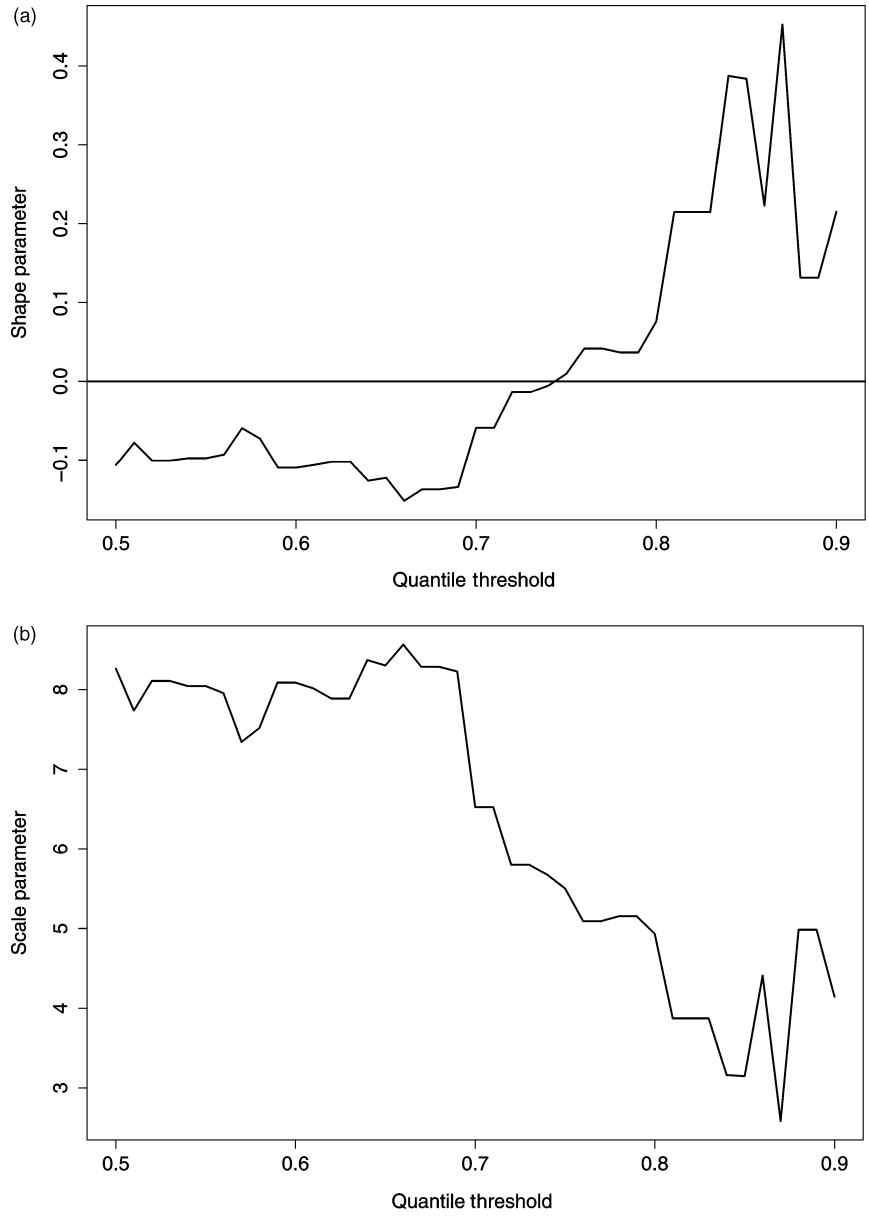

Figure 6. (a) Variation of the shape parameter ξ, and (b) the scale parameter σ for different choices of quantiles in a locally fitted polynomial quantile regression model.

7. Summary and discussion

The annual melt-season length τ has been computed on the basis of reconstructed daily temperature values at the Svalbard airport from 1912 to 2010. With segmented linear trend analysis, a positive trend in the period 1912–1929 (0.95 ± 0.46 days/year), a slightly decreasing trend in the period 1930–1985 (-0.09 ± 0.08 days/year) and a new increasing trend in the period 1986–2010 (1.11 ± 0.28 days/year) was found, demonstrating large decadal variation. Use of a linear regression model with the annual Northern Hemispheric temperature anomaly (T_{gnh}), annual regional SST anomaly (SST) and the seasonal NAO index (Li and Wang, 2003) as predictors explained 40% of the variance. SST and T_{gnh} were the most important factors in explaining changes in τ. These were followed in importance by the summer NAO index and the preceding winter NAO index. A model for extreme values of τ using GPD was used to assess the risk of extremely long melt seasons. SST and T_{gnh} turned out to be the only useful covariates, and the variability of long melt seasons increased with higher T_{gnh} and SST. The 100-year return level of τ changed from 131 (108, 138) days for $T_{gnh} = 0\,^{\circ}\mathrm{C}$ and $SST = 0\,^{\circ}\mathrm{C}$ to 153 (98, 206) days for $T_{gnh} = 1\,^{\circ}\mathrm{C}$ and $SST = 0\,^{\circ}\mathrm{C}$. In the case $T_{gnh} = 1\,^{\circ}\mathrm{C}$ and $SST = 1\,^{\circ}\mathrm{C}$, the 100-year return level of τ raised to 175 (109, 242) days. However, the results with $T_{gnh} > 0.5\,^{\circ}\mathrm{C}$ must be interpreted with caution, due to potential extrapolation errors. Nevertheless, these results indicate that large changes in the melt-season length might occur with a one-degree warming in global temperature and regional SST. The relative strength of individual physical mechanisms might change, but this

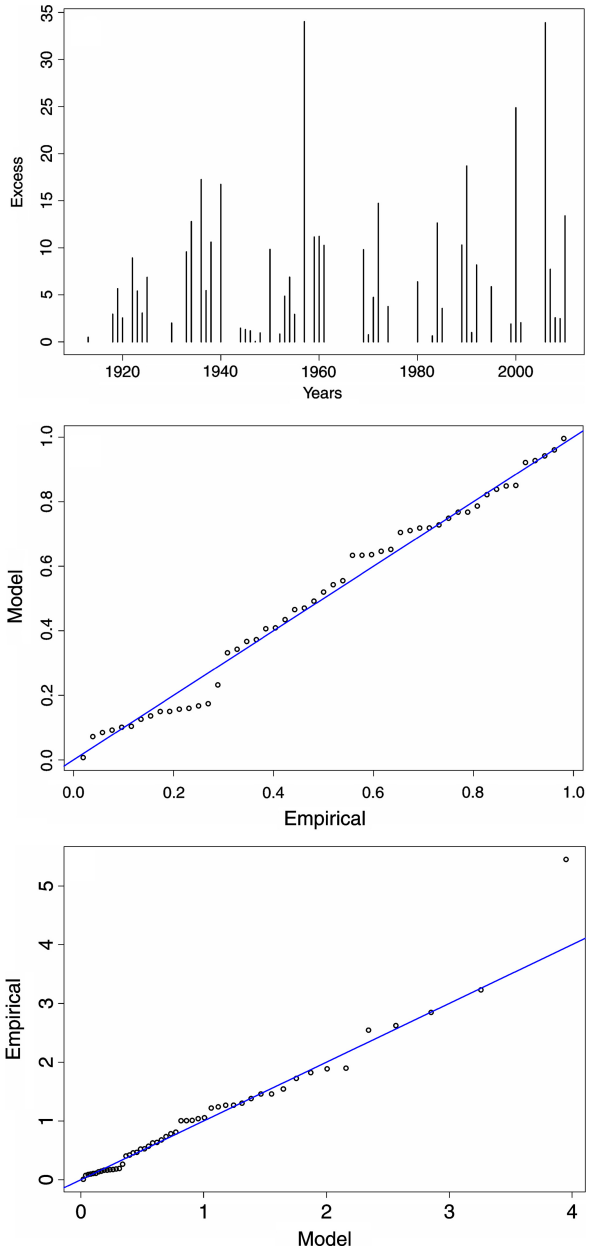

Figure 7. (a) Melt-season length excesses with the 70% time varying threshold. (b) Probability plot where the x-axis is the rank of the excesses divided by the total number of excesses. The y-axis denotes the cumulative distribution of the standardized excesses. (c) Quantile plot where the logarithms of the excesses are along the x-axis and standardized excesses are along the y-axis. This figure is available in colour online at wileyonlinelibrary.com/journal/joc

may nevertheless indicate how τ develops in a future climate.

As mentioned in Section 1, the homogenized monthly time series at Svalbard airport (Nordli and Kohler, 2004, 2010) was used to reconstruct daily temperature values in the period from 1912 to 2006. The time series was reconstructed from several shorter series of measurements at a few nearby sites. This composite could potentially have errors caused by the adjustment of many series. This is especially true for the period from 1912 to 1920, when there was a dramatic increase in annual mean temperature. Comparisons with ice core data showed that the winters in that period might have been warmer than indicated by the Svalbard airport time series (Kohler *et al*., 2003), implying that the first years of the record may not be trusted to the same degree. When the years 1912–1920 were excluded, our main conclusions remained the same. Changes in the instrumentation and vegetation could also have had an influence on the temperature record (Peterson *et al*., 1998).

One of the major problems with analysing the climate of the high Arctic is the absence of long-lasting datasets (Przybylak, 2003). The time series for Svalbard airport is one of the longest available. A new gridded dataset for the Arctic in the period 1900–2000 was recently presented by Kuzmina *et al*. (2008), and the methods used in our study can be expanded to this gridded dataset. Preliminary tests with gridded daily 10-m temperatures from ERA-40 reanalysis data (Kållberg *et al*., 2004) for the period 1958–2001 indicates this (not shown). For some regions, such as the North Atlantic sector, there was a strong positive correlation with T_{gnh}, while this correlation was weaker and even negative in other regions (e.g. south of Greenland). However, the ERA-40 data were for a short period (43 years), and the results are, therefore, statistically less significant. This also addresses the need to explore other predictors that can be used in statistical modelling of the melt season.

The alternative method of GPD, a block design approach that utilizes a general extreme value (GEV) distribution, could also be applied to the data. For annual observations of τ, decades could be thought of as a block size. However, with only ten observations, the blocks are normally not considered large enough. Larger blocks (e.g. a few decades) would imply that already small sample sizes of estimation for GEV parameters are even more reduced. Therefore, the peak-over-threshold approach is preferred. However, there is an issue as to how high the threshold should be. According to IPCC WG1 (2001), extremes should be accounted for events higher than the 90th or lower than the 10th quantile. In this study, the 70th quantile was chosen. The time series of τ was short, and the asymptotic assumption of the EVT model requires a lower choice of threshold, compared to that suggested by the IPCC WG1 (2001). Because τ is a seasonal variable, a high threshold like the 90th quantile will result in few excesses. Tests with higher thresholds (e.g. 80th and 90th quantile) showed that the T_{gnh} in general still influenced the variability of the extremes. However, the shape of the GPD distribution changed from negative to positive, making it difficult to estimate a theoretical upper limit of the excesses. The probability and quantile plots (Figure 7) also showed larger deviations from linearity with higher thresholds. Another issue is that τ is not stationary in time. This makes it necessary to fit a time-varying threshold, as introduced earlier in Coelho *et al*. (2008). A nonlinear quantile regression (Koenker, 2005) has been introduced as a simple method for estimation of the threshold, with the potential to be used in gridded datasets. Another approach is to detrend τ in time and

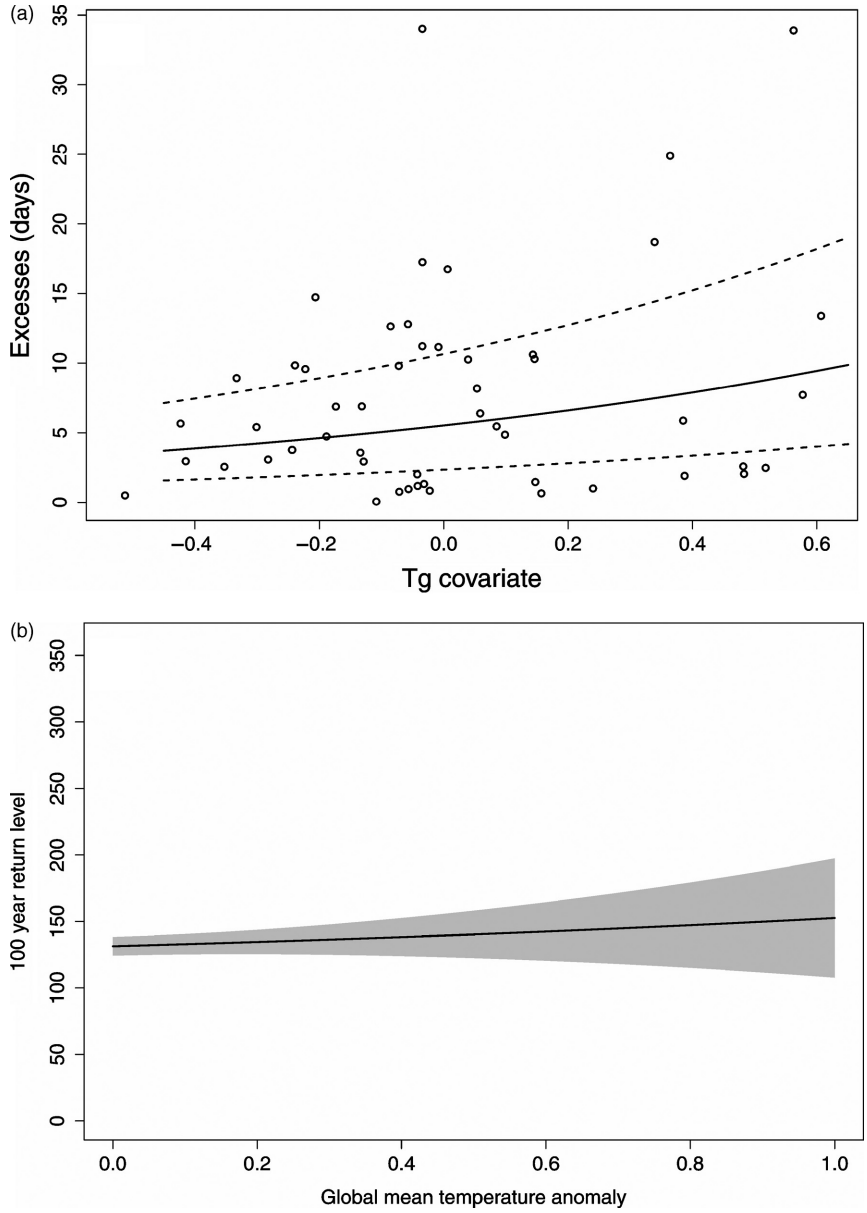

Figure 8. (a) Scatter plot of the excesses and Northern Hemisphere mean temperature anomalies (T_{gnh}). Solid line: Median. Dashed lines: Upper and lower quartiles of the GPD distribution using the estimated scale and shape parameters in Equations (4) and (5). (b) The return level of 100-year events (y-axis) and T_{gnh} (x-axis). The 95% confidence level (shaded area) was calculated based on the delta method (Coles, 2001 (p. 33)).

use a constant threshold. This was tested in the present research, but yielded no changes to our main conclusions.

Acknowledgements

This study was supported by EU-project ENSEMBLES (GOCECT- 2003-505539). We thank Chris Ferro for very valuable discussions regarding EVT theory, and also Carlo Casty for providing data. We also thank two anonymous reviewers for insightful comments to the manuscript.

References

ACIA. 2005. *Arctic Climate Impact Assessment – Scientific Report*. Cambridge University Press. ISBN:9780521865098, DOI: 10.2277/0521865093.

Alexeev VA, Langen PL, Bates JR. 2005. Polar amplification of surface warming on an aquaplanet in "ghost forcing" experiments without sea ice feedbacks. *Climate Dynamics* **24**: 655–666, DOI: 10.1007/s00382-005-0018-3.

Azen R, Budescu DV. 2006. Comparing predictors in multivariate regression models: An extension of dominance analysis. *Journal of Educational and Behavioral Statistics* **31**(2): 157–180.

Barnston AG, Livezey RE. 1987. Classification, seasonality and persistence of low-frequency atmospheric circulation patterns. *Monthly Weather Review* **115**: 1083–1126.

Belchansky G, Douglas DC, Platonov NG. 2004. Duration of the Arctic Sea ice melt season: Regional and interannual variability, 1979–2001. *Journal of Climate* **17**(1): 67–80.

Bengtsson L, Semenov VA, Johannessen OM. 2004. The Early Twentieth-Century Warming in the Arctic – A possible Mechanism. *Journal of Climate* **17**(10): 4045–4057.

Budescu DV. 1993. Dominance analysis: A new approach to the problem of relative importance of predictors in multiple regression. *Psychological Bulletin* **114**(3): 542–551.

Casty C, Raible CC, Stocker TF, Wanner H, Luterbacher J. 2007. A European pattern climatology 1766–2000. *Climate Dynamics* **29**(7): 791–805.

Cleveland WS. 1979. Robust locally weighted regression and smoothing scatterplots. *Journal of the American Statistical Association* **74**: 829–836.

Cleveland WS. 1981. LOWESS: A program for smoothing scatterplots by robust locally weighted regression. *The American Statistician* **35**: 54.

Coelho CAS, Ferro CAT, Stephenson DB, Steinskog DJ. 2008. Methods for exploring spatial and temporal variability of extreme events in climate data. *Journal of Climate* **21**(10): 2072–2092.

Coles S. 2001. *An Introduction to Statistical Modeling of Extreme Values*. *Springer Series in Statistics*. Springer Verlag. 1st Edition., 2001, XIV, ISBN 978-1-85233-459-8.

Comisio J. 2003. Warming trends in the Arctic from clear sky satellite observations. *Journal of Climate* **16**(21): 3498–3510.

de Boor C. 1979. *A practical guide to splines, Applied mathematical sciences*, vol 27, Academic Press, ISBN 978-0-387-95366-3.

Epstein ES. 1991. On obtaining daily climatological values from monthly means. *Journal of Climate* **4**(3): 365–368.

Foster JL, Robinson DA, Hall DK, Estilow TW. 2008. Spring snow melt timing and changes over Arctic lands. *Polar Geography* **31**(3): DOI: 10.1080/10889370802580185.

Francis JA, Hunter E. 2006. New insight into the disappearing Arctic sea ice. *Eos Transactions AGU* **87**: 509.

Francis JA, Hunter E. 2007. Drivers of declining sea ice in the Arctic winter: A tale of two seas. *Geophysical Research Letters* **34**(17): L17503.

Green PJ, Silverman BW. 1993. *Nonparametric Regression and Generalized Linear Models: A Roughness Penalty Approach.* Chapman & Hall/CRC.

Hartmann D.L. 1994. *Global physical climatology. International Geophysics series*, volume 56. Academic Press, 412 pp.

Hatzianastassiou N, Matsoukas C, Fotiadi A, Pavlakis KG, Drakakis E, Hatzidimitriou D, Vardavas I. 2005. Global distribution of Earths surface shortwave radiation budget. *Atmospheric Chemistry and Physics* **5**: 28472867.20.

Hinzman LD, Bettez ND, Bolton WR, Chapin FS, Dyurgerov MB, Fastie CL, Griffith B, Hollister RD, Hope A, Huntington HP, Jensen AM, Jia GJ, Jorgenson T, Kane DL, Klein DR, Kofinas G, Lynch AH, Lloyd AH, McGuire AD, Nelson F, Oechel WC, Osterkamp TE, Racine CH, Romanovsky VE, Stone RS, Stow DA, Sturm M, Tweedie CE, Vourlitis GL, Walker MD, Walker DA, Webber PJ, Welker JM, Winker K, Yoshikawa K. 2005. Evidence and implications of recent climate change in northern Alaska and other Arctic regions. *Climatic Change* **72**: 251–298.

IPCC WG1. 2001. Houghton JT, Ding Y, Griggs DJ, Noguer M, van der Linden PJ, Dai X, Maskell K, Johnson CA, (ed). *Climate Change 2001: The Scientific Basis, Contribution of Working Group I to the Third Assessment Report of the Intergovernmental Panel on Climate Change*, Cambridge University Press, ISBN 0-521-80767-0 (pb: 0-521-01495-6).

IPCC WG2. 2001. McCarthy JJ, Canziani OF, Leary NA, Dokken DJ, White KS, (ed.) *Climate Change 2001: Impacts, Adaptation and Vulnerability, Contribution of Working Group II to the Third Assessment Report of the Intergovernmental Panel on Climate Change*, Cambridge University Press, ISBN 0-521-80768-9 (pb: 0-521-01500-6).

IPCC WG1 AR4. 2007. Solomon S, Qin D, Manning M, Chen Z, Marquis M, Averyt KB, Tignor M, Miller HL. (ed). *Climate Change 2007*: *The Physical Science Basis, Contribution of Working Group I to the Fourth Assessment Report of the Intergovernmental Panel on Climate Change*, Cambridge University Press, ISBN 978-0-521-88009-1 (pb: 978-0-521-70596-7).

IPCC WG2 AR4. 2007. Parry ML, Canziani OF, Palutikof JP, van der Linden PJ, Hanson CE. (ed). *Climate Change 2007: Impacts, Adaptation and Vulnerability, Contribution of Working Group II to the Fourth Assessment Report of the Intergovernmental Panel on Climate Change*, Cambridge University Press, ISBN 978-0-521-88010-7 (pb: 978-0-521-70597-4).

Johannessen OM, Pettersson LH. 2008. *Arctic climate and shipping. In High North High Stakes*. Gottemoeller R, Tamnes R (Eds). Fagbokforlaget. pp. 95–114.

Jones PD, New M, Parker DE, Martin S, Rigor IG. 1999. Surface air temperature and its variations over the last 150 years. *Reviews of Geophysics* **37**: 173–199.

Kallberg P, Simmons A, Uppala S, Fuentes M. 2004. The ERA-40 archive. Reading, UK, European Centre for Medium-range Weather Forecasts (ECMWF), ECMWF Re-Analysis Project (ERA), 2004. 31p. ERA-40, *Project Report Series*, 17.

Kaufman DS, Schneider DP, McKay NP, Ammann CM, Bradley RS, Briffa KR, Miller GH, Otto-Bliesner BL, Overpeck JT, Vinther BM, Arctic Lakes 2k Project Members. 2009. Recent warming reverses long-term Arctic cooling. *Science* **325**: 1236–1239, DOI: 10.1126/science.1173983.

Koenker R. 2005. *Quantile Regression*. Econometric SocietyMonographs: Cambridge University Press.

Kohler J, Nordli Ø, Isaksson E, Pohjola V. 2003. Extending the 20th century temperature and precipitation records on Svalbard using newly available instrumental and ice-core data, *EGS – AGU – EUG Joint Assembly*. Abstracts from the meeting held in Nice, France, 6–11 April 2003, abstract #13555 pp. 13555.

Kuzmina SI, Johannessen OM, Bengtsson L, Aniskina OG, Bobylev LP. 2008. High northern latitude surface air temperature: comparison of existing data and creation of a new gridded data set 1900–2000. *Tellus Series A, Dynamic Meteorology and Oceanography* **60**(2): 289–304.

Li J, Wang J. 2003. A new North Atlantic Oscillation index and its variability. *Adv. Atmos. Sci.*, **20**(5): 661–676.

Loeng H, Brander K, Carmack E, Denisenko S, Drinkwater K, Hansen B, Kovacs K, Livingston P, McLaughlin F, Sakshaug E. 2005. Marine systems. *Arctic Climate Impact Assessment, ACIA*, Symon C, Arris L, Heal B (eds). Cambridge University Press, Cambridge: 453–538.

Markus T, Stroeve JC, Miller J. 2009. Recent changes in Arctic sea ice melt onset, freezeup, and melt season length. *Journal of Geophysical Research* **114**: C12024, DOI: 10.1029/2009JC005436.

Mesquita MDS. 2006. *Tracking Summer Extra-Tropical Storms: A climatological overview and variability in the North Atlantic*. Master Thesis in Climatology, Geophysical Institute, University of Bergen.

Muggeo VMR. 2003. Estimating regression models with unknown breakpoints *Statistics in Medicine* **22**: 3055–3071.

Naveau P, Nogaj M, Ammann C, Yiou P, Cooley D, Jomelli V. 2005. Statistical methods for the analysis of climate extremes. *Comptes Rendus Geoscience* **337**: 1013–1022.

Nogaj M, Yiou P, Parey S, Malek F, Naveau P. 2006. Amplitude and frequency of temperature extremes over the North Atlantic region. *Geophysical Research Letters* **33**: L10801.

Nicolaus Copernicus University Institute of Geography Gagarina 9, 87-100 Torun?, Poland http://www.zklim.umk.pl/en/bulletin-of-geography/

Nordli Ø, Kohler J. 2004. The early 20th century warming. In *Daily Observations at Grønfjorden and Longyearbyen on Spitsbergen*. Norwegian Meteorological Institute: Oslo.

Peterson TC, Easterling DR, Karl TR, Groisman P, Nicholls N, Plummer N, Torok S, Auer I, Boehm R, Gullett D, Vincent L, Heino R, Tuomenvirta H, Mestre O, Szentimrey T, Salinger J, Forland EJ, Hanssen-Bauer I, Alexandersson H, Jones P, Parker D. 1998. Homogeneity adjustments of in situ atmospheric climate data: A review. *International Journal of Climatology* **18**(13): 1493–1517.

Polyakov IV, Alekseev GV, Bekryaev RV, Bhatt U, Colony RL, Johnson MA, Karklin V, Makshtas AP, Walsh D, Yulin AV. 2002. Observationally based assessment of polar amplification of global warming. *Geophysical Research Letters* **19**(18): 1878.

Polyakov IV, Bekryaev RV, Alekseev GV, Bhatt US, Colony RL, Johnson MA, Maskshtas AP, Walsh D. 2003. Variability and trends of air temperature and pressure in the maritime Arctic, 1875–2000. *Journal of Climate* **16**(12): 2067–2077.

Przybylak R. 2003. *The Climate of the Arctic*. *Atmospheric and Oceanographic Sciences Library*. Kluwer Academic Publishers, Dordrecht, Netherlands.

Ramanathan V, Barkstrom BR, Harrison EF. 1989. Climate and the Earths radiation budget. *Physics Today* **42**(5): 22–32.

Rayner NA, Parker DE, Horton EB, Folland CK, Alexander LV, Rowell DP, Kent EC, Kaplan A. 2003. Global analyses of sea surface temperature, sea ice, and night marine air temperature since the late nineteenth century *Journal of Geophysical Research* **108**(D14): 4407 10.1029/2002JD002670.

Rigor IG, Colony RL, Martin S. 2000. Variations in surface air temperatures in the Arctic, 1979-97. *Journal of Climate* **13**: 896–914.

Schwartz SE. 2007. Heat capacity, time constant, and sensitivity of Earth's climate system. *Journal of Geophysical Research-Atmospheres* **112**(D24): D24S05.

Seierstad IA, Stephenson DB, Kvamstø NG. 2007. How useful are teleconnection patterns for explaining variability in extratropical

storminess? *Tellus Series A, Dynamic Meteorology and Oceanography* **59**(2): 170–181.

Serreze MC, Barrett AP, Slater AG, Steele M, Zhang J, Trenberth KE. 2007. The large-scale energy budget of the Arctic. *Journal of Geophysical Research* **112**: D11122, DOI: 10.1029/2006JD008230.

Serreze MC, Barrett AP, Stroeve JC, Kindig DN, Holland MM. 2009. The emergence of surface-based Arctic amplification. *Cryosphere* **3**: 11–19, DOI: 10.5194/tc-3-11-2009.

Serreze MC, Walsh JE, Chapin FS, Osterkamp T, Dyurgerov M, Romanovsky V, Oechel WC, Morison J, Zhang T, Barry RG. 2000. Observational evidence of recent change in the northern high-latitude environment. *Climatic Change* **46**(1): 159–207.

Smedsrud LH, Sorteberg A, Kloster K. 2008. Recent and future changes of the Arctic sea-ice cover. *Geophysical Research Letters* **35**: L20503, DOI: 10.1029/2008GL034813.

Sorteberg A, Furevik T, Drange H, Kvamstø NG. 2005. Effects of simulated natural variability on Arctic temperature projections. *Geophysical Research Letters* **32**: L18708, DOI: 10.1029/2005GL023404.

Sorteberg A, Kvamstø NG. 2006. The effect of internal variability on anthropogenic climate projections. *Tellus* **58A**: 565–574, DOI: 10.1111/j.1600-0870.2006.00202.x.

Smith NV, Saatchi SS, Randerson JT. 2004. Trends in high northern latitude soil freeze and thaw cycles from 1988 to 2002. *Journal of Geophysical Research* **109**: D12101.

Sorteberg A, Kvingedal B. 2006. Atmospheric forcing on the Barents Sea Winter Ice Extent. *Journal of Climate* **18**(10): 4772–4784.

Wallace JM, Gutzler DS. 1981. Teleconnections in the Geopotential Height Field during the Northern Hemisphere winter. *Monthly Weather Review* **109**: 784–812.

